CORROSION SCIENCE AND TECHNOLOGY, Vol.23, No.6(2024), pp.556~561 pISSN 1598-6462 / eISSN 2288-6524
[Research Paper] DOI: https://doi.org/10.14773/cst.2024.23.6.556

Antiviral Steel Sheets Effective Against SARS-CoV-2

Fumio Shibao†

East Nippon R&D Laboratory, Nippon Steel Corporation, 1 Kimitsu, Kimitsu-shi, Chiba 299-1141, Japan
(Received January 11, 2024; Revised April 22, 2024; Accepted May 01, 2024)

In recent years, the awareness of infection prevention has increased owing to the spread of the novel coronavirus disease 2019. Antiviral products are necessary to avoid the risk of infection from existing and new SARS-CoV-2 variants. There is a growing need to impart antiviral properties to applications involving human contact. Therefore, antiviral steel sheets with a visible-light-responsive photocatalyst in the surface layer were developed in this study with intended applications on office furniture and interior finishing of buildings frequently touched by numerous people. The antiviral effect was investigated using a non-enveloped bacteriophage Q-beta (lipid bilayer membrane) and an enveloped SARS-CoV-2. A series of antiviral tests were conducted in compliance with JIS R 1756:2020 or by applying mutatis mutandis. Resistance of these antiviral steel sheets to sunlight was also investigated. These antiviral steel sheets developed in this study exhibited fingerprint resistance, formability, and antiviral properties. These sheets were also durable under exposure to sunshine. Thus, they can be used as an effective tool to reduce the risk of SARS-CoV-2 infection.

Keywords: *Antiviral, Photocatalyst, Visible light responsibility, Steel sheet, SARS-CoV-2*

1. Introduction

The novel coronavirus disease 2019 (COVID-19) has spread worldwide since the end of 2019, and emerged as a pandemic. The severe acute respiratory syndrome coronavirus 2 (SARS-CoV-2) has mutated repeatedly, and the Delta and Omicron strains have become prevalent strains worldwide. As of June 2023, when this report was prepared, the COVID-19 pandemic had subsided. However, the risk of infection persists, owing to new mutant strains, and should be considered for adequate public health management. Vaccination, air-conditioning management [1], use of masks, and adequate disinfection are used to reduce these risks. For example, SARS-CoV-2 and influenza viruses are inactivated by alcohols and cationic surfactants [2,3]. Moreover, as viruses cannot replicate outside the body, methods that prevent them from adhering to the surface of substances are being studied to block their route of entry into the body [4]. However, most measures become less effective over time and require regular surface treatments.

This study focused on photocatalysts as materials that can sustainably exhibit antiviral properties. When light irradiates a photocatalyst, electrons are excited and move to the conduction band. Holes are formed by the movement of electrons, and are positively charged. The electrons are negatively charged. These holes take electrons from the hydroxyl ions in water and produce hydroxyl radicals. Electrons react with oxygen in the air to produce oxygen radicals [5]. These radicals have a strong oxidizing effect and disrupt the viral envelope and outer shell. Consequently, the virus is deactivated. Photocatalysts exhibit oxidizing effects when they absorb light sustainably.

This study developed antiviral steel sheets suitable for surfaces touched by several people, such as office furniture and internal surfaces in buildings. Therefore, fingerprint resistance and good formability in press forming are required apart from good appearance and antiviral properties. The top coat of these products contains a visible light-responsive photocatalyst that exhibits a strong oxidative effect even under the illuminance of indoor lighting levels and exerts an antiviral effect. The material also has a hybrid function that exerts this effect even in the dark.

†Corresponding author: shibao.a63.fumio@jp.nipponsteel.com

2. Experimental Methods

2.1 Specimens

Antiviral steel sheets with visible light-responsive photocatalysts on their outermost surface were fabricated based on two types of designable steel sheets. Fig. 2 shows the cross-sectional structures of the developed samples A and B, with Zn-plated steel sheets as the base material. Sample A had an electroplated Zn–Ni alloy hairline on the surface, producing a metallic design. Zn-Ni plating was selected to achieve a brightness similar to that of hairline stainless steel [6]. Unlike its conventional variant, sample A had a topcoat with visible light-responsive photocatalysts. The radicals generated by the photocatalyst decomposed the surrounding organic matter. Therefore, an inorganic film that suppressed self-attack by the photocatalyst was used as the chemical conversion treatment film for Sample A. Sample B was a pre-coated steel sheet with a hot-dip galvanized steel sheet as the base plate, which could be adjusted to any color using the pigments in the resin coatings. The resin film was made of polyester/melamine-formaldehyde, which has high processability. A white pigment was used for coloring both samples. Unlike its conventional variant, sample B had a topcoat with visible light-responsive photocatalysts and a barrier coat. To prevent self-attack by the photocatalyst, a barrier layer made of an inorganic film was provided to sample B so that the coating film and the photocatalyst did not come into contact.

2.2 Antiviral effect

A series of antiviral tests were conducted in compliance with Japanese Industrial Standards (JIS) R 1756:2020 (fine ceramics determination of the antiviral activity of photocatalytic materials under indoor lighting environment test method using bacteriophage Q-beta), or through mutatis mutandis. The illuminance at the time of the test was set at 500 lx (equivalent to a dark environment). The test times were 0, 5, 30, 60, 120, and 240 min. The antiviral steel sheets shown in Fig. 1 were used as the object specimens, and conventional steel sheets without a photocatalyst were used as comparative specimens. The antiviral effect was evaluated assuming that the plaque-forming units (PFU) determined after the test using the plaque method were equal to the number of viruses; the viral detection limit was 10.

Antiviral effect was investigated using the bacteriophage Q-beta without an envelope (lipid bilayer membrane), as required by JIS R 1756:2020, and SARS-CoV-2 with an envelope. Viruses without an envelope are generally considered to be more resistant to disinfectants than those with an envelope [7]. Therefore, the antiviral effect confirmed for Q-beta, a virus without an envelope, should be effective against SARS-CoV-2, a virus with an envelope. Additionally, we conducted an antiviral test using SARS-CoV-2 to confirm the efficacy against COVID-19.

At 500 lx brightness, used in living rooms, dining rooms, kitchens, bathrooms, offices, conference rooms, and classrooms, simple work can be performed [8]. Most home appliances, furniture, and walls touched daily are under illuminated environments of ≥ 500 lx. The viral reduction rate was determined using Equation 1. When the number of viruses was below the detection limit (10), it was set as 10.

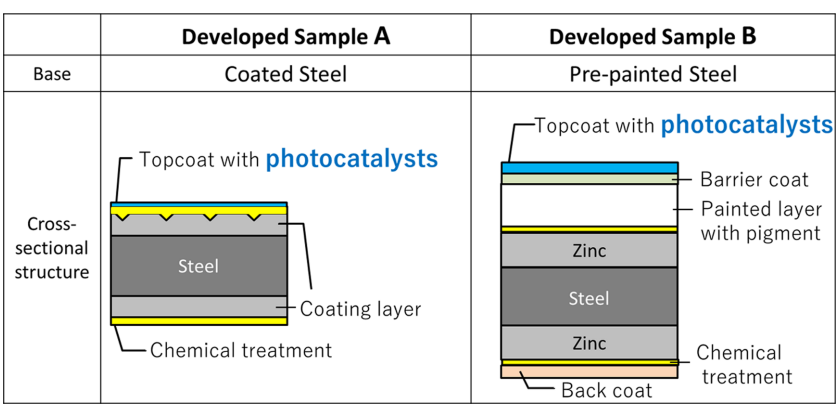

Fig. 1. Cross-sectional structure of the antiviral steel sheets

Virus reduction rate = $(N_C\text{-}N_D) / N_C$ (1)

N_C: Number of viruses on the conventional sample
N_D: Number of viruses on the developed sample

2.3 Durability

The durability of the antiviral steel sheets was investigated based on their antiviral abilities after weather resistance testing. If the developed samples are exposed to intense light, such as sunshine, the topcoat may decompose because of the strong oxidation of the photocatalyst. Consequently, the photocatalyst might wear off, resulting in reduced antiviral abilities and peeling of the paint film.

Therefore, the durability of the antiviral steel sheets after solar irradiation was assessed. Weather resistance tests were conducted for 250 h using a sunshine weather meter (SWOM S80; Suga Test instruments Co., Ltd., Tokyo, Japan). Subsequently, antiviral properties were investigated using the method described in section 2.2. The adhesion of the coating film after the SWOM test was investigated using a crosscut test (JIS K 5400-8.5).

2.4 Fingerprint resistance

Antiviral steel sheets are intended for applications in which they are touched by human hands; however, their appearance can deteriorate if fingerprints remain on the structure. Therefore, the fingerprint resistance of the products was examined. The test pieces were immersed for 5 s in an acetone solution containing 0.5 mass% white petrolatum, and the appearance before and after immersion was evaluated visually and in terms of color difference (ΔE*), which was calculated by measuring the color tone (L*, a*·b*) using a colorimeter (CR-400; Konica Minolta, Inc. Tokyo, Japan), using Equation 2. Conventional samples (without the photocatalyst) were used for comparison.

$$\Delta E^* = ((L_1^* - L_2^*)^2 + (a_1^* - a_2^*)^2 + (b_1^* - b_2^*)^2)^2 \quad (1)$$

where L_1^*, a_1^*, and b_1^* are the color tones before immersion, and L_2^*, a_2^*, and b_3^* are the color tones after immersion in the white petrolatum solution.

2.5 Formability

Antiviral steel sheets were formed into final products by pressing, and their formability was tested. The specimens were subjected to cylindrical drawing using dies with inner diameters of 50 mm and shoulder radii of 5 mm. The drawing ratio was set at 2.0. After pressing, a crosscut was inscribed on the body surface with a cutter. The pieces were immersed in boiling water for 1 h, and a peeling test of the crosscut portion was conducted using adhesive tape. Conventional samples (without the photocatalyst) were used for comparison.

3. Results and Discussion

3.1 Antiviral effect

Fig. 2 shows the antiviral effect of sample A against Q-beta. The test time was 240 min. In the dark, the number of viruses on sample A was lesser than that on the corresponding conventional sample without a photocatalyst by 99.9%. At 500 lx illuminance, the number of viruses on sample A reduced below the detection limit (10 at most), which was less than that on the corresponding conventional sample by ≥ 99.99%. These results indicate that sample A exerts an antiviral effect in both dark and

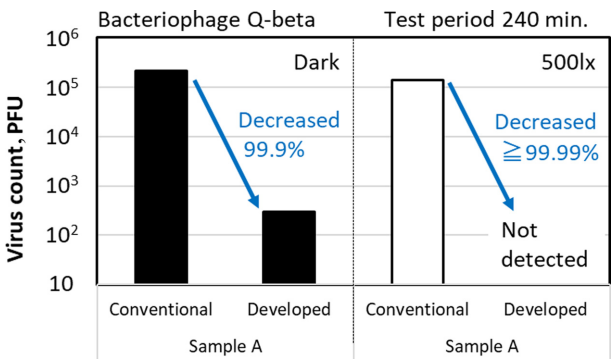

Fig. 2. Antiviral effect of sample A against Q-beta

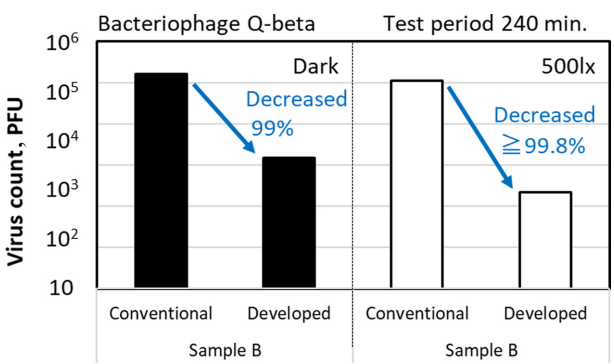

Fig. 3. Antiviral effect of sample B against Q-beta

light environments, exhibiting a hybrid function, and the antiviral effect in light environments was higher than that in the dark.

Fig. 3 shows the antiviral effect of sample B against Q-beta. Similar to sample A, it exhibited an antiviral effect both in dark and light conditions. In addition, it exhibited higher antiviral activity under light than under dark conditions.

Fig. 4 shows the antiviral activity of sample A against SARS-CoV-2. The test time was 240 min. In the dark, the number of viruses on sample A reached the detection limit; the number of viruses on sample A was lesser than that on the comparative sample by ≥ 99.5%. Under 500 lx illuminance, the virus count on sample A was below the detection limit, which was less than that on the comparative sample by ≥ 99.8%.

The antiviral test results shown in Figs. 2 and 4, demonstrate that there were fewer SARS-CoV-2 than Q-beta on the tested samples. This result is consistent with previous studies [7].

Fig. 5 shows the relationship between the antiviral test time and the number of viruses. At 500 lx illuminance, compared to the corresponding conventional sample, the Q-beta count on sample A decreased by 99% after testing for 5 and 30 min, 99.9% after 60 min, and 99.99% after 120 min. These results confirmed the antiviral effect of sample A within a short period.

3.2 Durability

Fig. 6 shows the antiviral effect of sample A against Q-beta after the SWOM test (240 min; 500 lx illuminance). The number of viruses on sample A was lesser than that on the corresponding conventional sample by 99.9%. This indicated that sample A exhibited antiviral activity even after the weather resistance test.

Fig. 7 shows the antiviral effect of Sample B against Q-beta after the SWOM test (240 min; 500 lx illuminance). The number of viruses on sample B was lesser than that on the corresponding conventional sample by 99.9%. This

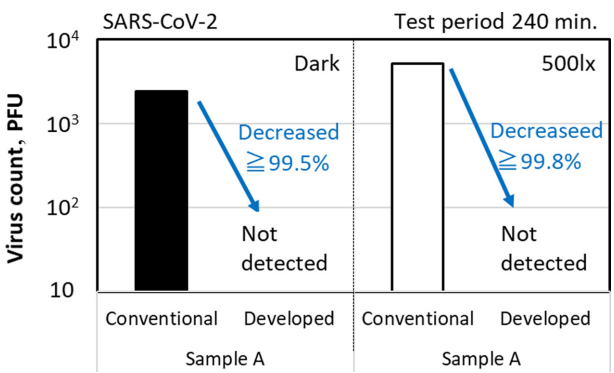

Fig. 4. Antiviral effect of sample A against SARS-CoV-2

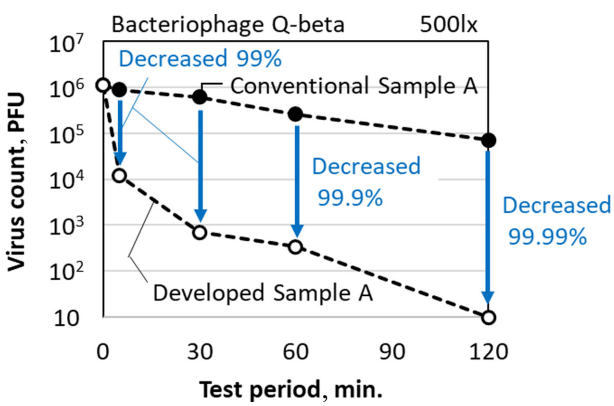

Fig. 5. Association between test period and virus count for sample A, using Q-beta

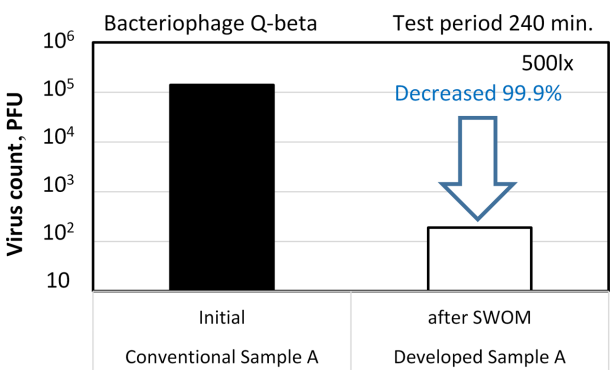

Fig. 6. Antiviral effect of sample A against Q-beta after the SWOM test

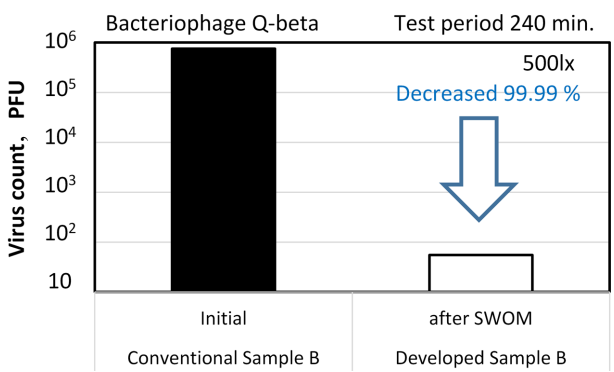

Fig. 7. Antiviral effect of sample B against Q-beta after the SWOM test

Table 1. Results of the adhesion test

Specimens		Adhesion
Developed Sample A	After SWOM	10 (No peeling)
Conventional Sample A	Initial	10 (No peeling)
Developed Sample B	After SWOM	10 (No peeling)
Conventional Sample B	Initial	10 (No peeling)

Table 2. Results of fingerprint resistance test

Specimens	Visual judgement	Color difference (ΔE*)
Developed Sample A	Invisible	0.8
Conventional Sample A	Invisible	1.0
Developed Sample B	Invisible	0.4
Conventional Sample B	Invisible	0.9

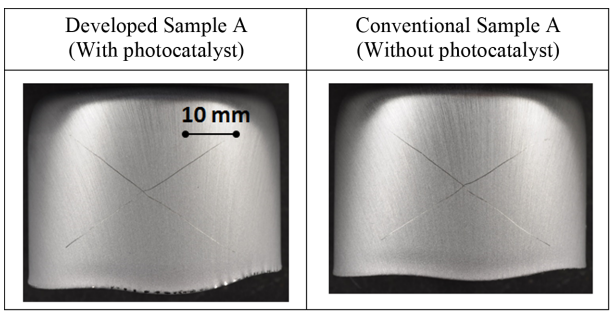

Fig. 8. Formability of sample A

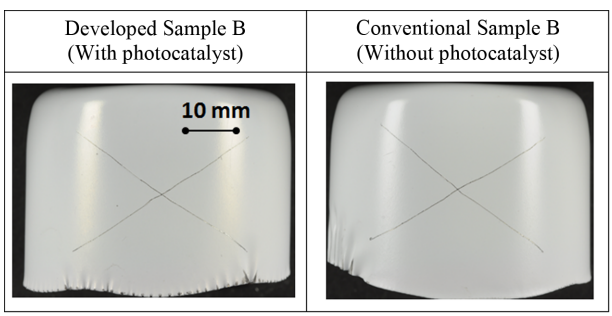

Fig. 9. Formability of sample B

indicated that sample B exhibited antiviral activity even after the weather resistance test.

Table 1 lists the adhesion test results obtained from the SWOM tests. Peeling of the coating film was not observed in either sample A or B.

Samples A and B were considered to exhibit sufficient durability, even when used in an environment with sunshine.

3.3 Fingerprint resistance

The results of the fingerprint resistance tests are presented in Table 2. Samples A and B exhibited the same fingerprint resistance as their corresponding conventional samples.

3.3 Formability

Fig. 8 shows the appearance of sample A and its corresponding conventional sample after the peeling test. No swelling or peeling of the coating film was observed at the crosscut, verifying that sample A had the same high formability as the conventional sample.

Fig. 9 shows the appearance of sample B and its corresponding conventional sample after the peeling test. No swelling or peeling of the coating film was observed at the crosscut, verifying that sample B had the same high formability as the conventional sample.

4. Conclusion

In this study, I evaluated the performance of antiviral steel sheets with visible light-responsive photocatalytic surface coatings. This antiviral steel sheet had a sufficient antiviral effect that was effective against SARS-CoV-2, and had the same fingerprint resistance and formability as conventional steel sheets. In addition, these antiviral steel sheets showed sufficient antiviral efficacy even after the durability test.

References

1. M. Hayashi, *Environment and Building Services*, **173**, 12 (2021). (in Japanese)
2. R. A. Leslie, S. S. Zhou, and D. R. Macinga, Inactivation of SARS-CoV-2 by commercially available alcohol-based hand sanitizers, *American journal of infection control*, **49**, 401 (2021). Doi: https://doi.org/10.1016/j.ajic.2020.08.020
3. P. I. Hora, S. G. Pati, P. J. McNamara, and W. A. Arnold, Increased Use of Quaternary Ammonium Compounds during theSARS-CoV-2 Pandemic and Beyond: Consideration of EnvironmentalImplications, *Environmental Science & Technology Letters*, **7**, 622 (2020). Doi: https://doi.org/10.1021/acs.estlett.0c00437
4. D. Campocciaa, L. Montanaroa, and C. R. Arciol, A review of biomaterials technologies for infection-resis-

tant surfaces, *Biomaterials*, **34**, 8533 (2013). Doi: https://doi.org/10.1016/j.biomaterials.2013.07.089

5. A. Fujishima and K. Honda, Electrochemical Photolysis of Water at a Semiconductor Electrode, *Nature*, **238**, 37 (1972). Doi: https://doi.org/10.1038/238037a0
6. T. Futaba, F. Shibao, Y. Uesugi, T. Yokomichi, K. Kume, K. Haruta, and Y. Tanaka, Electro Galvanized Steel Sheet with Hairline-like Appearance "FeLuce™", *NIPPON STEEL TECHCAL REPORT*, **129**, 24 (2023). https://www.nipponsteel.com/common/secure/en/tech/report/pdf/129-05.pdf
7. Y. Murofushi, *Engineering materials*, **69**, 55 (2021). (in Japanese)
8. The Illuminating Engineering Institute of Japan, *Technical Guide for Residential Lighting Design*, Tokyo (2019). (in Japanese)